

**LDA+DMFT computation of the electronic spectrum of NiO**X. Ren,<sup>1,\*</sup> I. Leonov,<sup>1</sup> G. Keller,<sup>1</sup> M. Kollar,<sup>1</sup> I. Nekrasov,<sup>2</sup> and D. Vollhardt<sup>1</sup><sup>1</sup>*Theoretical Physics III, Center for Electronic Correlations and Magnetism, University of Augsburg, 86135 Augsburg, Germany*<sup>2</sup>*Institute of Electrophysics, Ural Branch of Russian Academy of Science, 620016, Ekaterinburg, Russia*

(Received 13 June 2006; published 20 November 2006)

The electronic spectrum, energy gap and local magnetic moment of paramagnetic NiO are computed using the local density approximation plus dynamical mean-field theory (LDA + DMFT). To this end the noninteracting Hamiltonian obtained within the LDA is expressed in Wannier function basis, with only the five antibonding bands with mainly Ni *3d* character taken into account. Complementing it by local Coulomb interactions one arrives at a material-specific many-body Hamiltonian which is solved by DMFT together with quantum Monte Carlo (QMC) simulations. The large insulating gap in NiO is found to be a result of the strong electronic correlations in the paramagnetic state. In the vicinity of the gap region, the shape of the electronic spectrum calculated in this way is in good agreement with the experimental x-ray-photoemission and bremsstrahlung-isochromat-spectroscopy results of Sawatzky and Allen. The value of the local magnetic moment computed in the paramagnetic phase (PM) agrees well with that measured in the antiferromagnetic (AFM) phase. Our results for the electronic spectrum and the local magnetic moment in the PM phase are in accordance with the experimental finding that AFM long-range order has no significant influence on the electronic structure of NiO.

DOI: [10.1103/PhysRevB.74.195114](https://doi.org/10.1103/PhysRevB.74.195114)

PACS number(s): 71.27.+a, 71.30.+h, 79.60.-i

**I. INTRODUCTION**

NiO is a strongly correlated electron material with a large insulating gap of 4.3 eV and an antiferromagnetic (AFM) ordering temperature of  $T_N=523$  K. Conventional band theories which stress the delocalized nature of electrons cannot explain this large gap and predict NiO to be metallic.<sup>1</sup> On the other hand, spin-polarized band calculations—e.g., density functional calculations based on the local spin-density approximation<sup>2</sup> (LSDA)—which do find an AFM insulating ground state in NiO, produce a band gap and local magnetic moment which are considerably smaller than the experimental values. These facts are often taken as evidence for the inapplicability of conventional band theories to strongly correlated systems like NiO. Indeed, already a long time ago Mott<sup>3</sup> showed that NiO and similar insulators may be better understood within a real-space picture of the solid, where localized electrons are bound to atoms with incompletely filled shells. This leads to the formation of incoherent bands, the lower and upper Hubbard bands, which are separated by a correlation gap of the order of the local Coulomb repulsion  $U$ . For this reason NiO has long been viewed as a prototype “Mott insulator.”<sup>3,4</sup>

This view of NiO was later replaced by that of a “charge transfer insulator,”<sup>5</sup> after Fujimori and Minami had successfully explained the photoemission data in terms of a cluster model treated within the configuration-interaction method.<sup>6</sup> In particular, this interpretation was supported by the combined x-ray-photoemission (XPS) and bremsstrahlung-isochromat-spectroscopy (BIS) measurements of Sawatzky and Allen.<sup>7</sup> Within this new picture an additional ligand  $p$  band appears between the lower and upper Hubbard bands, and the insulating gap is formed between the ligand  $p$  band and the upper Hubbard  $d$  band. However, unless the  $p$ - $d$  hybridization is taken into account, this picture is still an oversimplification. Namely, the hybridization between

transition-metal  $d$  and ligand  $p$  states will lead to some  $d$ -electron features also in the upper valence bands. Indeed, subsequent studies suggested that the first valence peak is actually a bound state arising from the strong hybridization of Ni  $3d$  and O  $2p$  states,<sup>8,9</sup> such that NiO is close to the intermediate regime of the Zaanen-Sawatzky-Allen scheme.<sup>5</sup> Despite the success of the cluster approach it has apparent drawbacks since it neglects the band aspects of O  $2p$  states completely which are known to play an important role in NiO.<sup>8,10</sup> The translational symmetry has been taken into account to some extent within the cluster perturbation theory recently.<sup>11</sup> Another extension is the treatment of a larger cluster (Ni<sub>6</sub>O<sub>19</sub>) so that nonlocal charge transfer excitations can be identified.<sup>12</sup>

Since the cluster approach relies on adjustable parameters to fit the experimental spectrum, it is highly desirable to obtain a description of the electronic structure of NiO from first principles. Already within L(S)DA the O  $2p$  bands can be accounted for quite well.<sup>8</sup> Attempts to go beyond L(S)DA are based on the self-interaction-corrected density functional theory (SIC-DFT),<sup>13</sup> the LDA+ $U$  method,<sup>14</sup> and the GW approximation.<sup>15,16</sup> These methods represent corrections of the single-particle Kohn-Sham potential in one way or another and lead to substantial improvements over the L(S)DA results for the values of the energy gap and local moment. Within the SIC-DFT and LDA+ $U$  methods the occupied and unoccupied states are split by the Coulomb interaction  $U$ , whereas within the LSDA this splitting is caused by the Stoner parameter  $I$ , which is typically one order of magnitude smaller than  $U$ . Therefore, compared with the LSDA, the SIC-DFT and LDA+ $U$  methods capture more correctly the physics of transition-metal (TM) oxides and improve the results for the energy gap and local moment significantly. The GW method goes one step further by calculating the self-energy to lowest order in the screened Coulomb interaction  $W$ , and the obtained band structure shows better agree-

ment with angle-resolved photoemission spectra (ARPES).<sup>16</sup> Since then, a large number of studies of NiO have been performed along these lines,<sup>17–23</sup> differing in the basis used and/or the details of the approximations. However, in both SIC-DFT and LDA+U the self-energy is static—i.e., does not take correlation effects into account adequately and thus cannot give an accurate description of the electronic energy spectrum of this correlated material. As to the GW method, its practical applications to NiO indicate that, in general, it also cannot explain strong correlation effects sufficiently. Furthermore, different implementations of the GW scheme lead to quite different results<sup>15,16,22,23</sup> regarding the value of the insulating gap and the relative positions of the energy bands.

Thus, although considerable progress was made in the theoretical understanding of NiO from first principles, several important issues are still open: first of all, the agreement with electronic energy spectra is far from satisfactory. This is not really surprising since the self-energies employed in the previous approaches are either energy independent (i.e., genuine correlations are not included) or are obtained from approximations whose validity is not entirely clear. Second, since conventional first-principles calculations are not able to incorporate the strong local electronic correlations, they have, with only a few exceptions,<sup>24</sup> focused on the AFM ground state and hence attributed the insulating gap to the existence of long-range magnetic order. It is well known, however, that both the band gap and the local magnetic moment are essentially unchanged even above the Néel temperature.<sup>4</sup> Indeed, recent experiments showed that long-range magnetic order has no significant influence on the valence band photoemission spectra<sup>25</sup> and the electron density distributions.<sup>26</sup> These facts are evidence for the strongly localized nature of the electronic states in NiO and cannot be understood within a Slater-type, static mean-field theory of antiferromagnetism.<sup>27</sup> Apparently the AFM long-range order itself is not the driving force behind the opening of the insulating gap but is merely a concomitant phenomenon—i.e., a *consequence* of the correlation-induced insulating gap, rather than its origin. We are thus led to the question whether the properties of the strongly correlated, paramagnetic (PM) insulating state of NiO can be calculated within a theoretical framework—i.e., explicitly *explained*—even in the absence of long-range AFM order.

In this work, we therefore investigate the PM insulating phase of NiO using the LDA+DMFT approach. This computational scheme for the *ab initio* investigation of strongly correlated materials was developed during the last decade<sup>28–30</sup> and has led to important insights into the physics of strongly correlated electron materials; for reviews, see Refs. 31–35. The LDA+DMFT approach combines band structure theory within the local density approximation (LDA) with many-body theory as provided by dynamical mean-field theory (DMFT).<sup>36,37</sup> Within DMFT, a lattice model is mapped onto an effective impurity problem embedded in a medium which has to be determined self-consistently<sup>38</sup>—e.g., by quantum Monte Carlo (QMC) simulations.<sup>39</sup> This mapping becomes exact in the limit of infinite dimensions.<sup>40</sup>

The LDA+DMFT approach is a particularly suitable scheme also for the investigation of the electronic properties

of NiO. Namely, it takes into account both the material-specific aspects as well as the strong electronic correlations in NiO, thus having advantages that the previous methods lack. This approach has been used by Savrasov and Kotliar<sup>41</sup> to study the phonon spectrum of NiO and MnO. In this work we concentrate on the electronic spectrum.

The paper is organized as follows. In Sec. II the LDA+DMFT computational scheme for NiO is presented. The general idea of modeling NiO by a material-specific many-body Hamiltonian is discussed in Sec. II A. In Sec. II B the Wannier functions and single-particle Hamiltonian matrix are constructed within the LDA, and the correlations are included by DMFT (QMC) in Sec. II C. The results are discussed and compared with experiment in Sec. III, and finally we conclude this paper in Sec. IV.

## II. COMPUTATIONAL METHOD

### A. Description of NiO with a multiband Hubbard model

In practice, LDA calculations usually involve a large number of valence *s*, *p*, and *d* orbitals associated with all the atoms in the unit cell. Since multiorbital QMC calculations are computationally expensive, especially at low temperatures, not all of these orbitals can be included in the DMFT calculation. For this reason one needs to project out most of the orbitals except for the most relevant ones.

For a large number of transition-metal compounds, the most relevant orbitals responsible for the physical properties are the transition-metal valence *d* orbitals which are partially filled and are located around the Fermi level. However, for some materials—e.g., the late transition-metal oxides, which are either charge-transfer insulators or in the intermediate regime of the Zaanen-Sawatzky-Allen scheme<sup>5</sup>—the oxygen *2p* orbitals are as important as the transition-metal valence *d* orbitals, and hence have to be taken into account in the effective model Hamiltonian as well. Thus, in principle, the strong Coulomb interaction among the *d* electrons and the *p-d* hybridization should be included and investigated on the same level. In DMFT this would correspond to the investigation of a material-specific multiorbital version (five *d* orbitals and three *p* orbitals) of the periodic Anderson model with nearest-neighbor hybridization. Such a comprehensive DMFT treatment is very difficult to perform even at present. Therefore, as a first step we turn to an approximate, but useful, procedure: namely, we include the hybridization only implicitly in the construction of the set of Wannier functions as will be described below.<sup>42</sup> With this set of Wannier functions as a basis, we arrive at an effective multiband Hubbard model. The on-site Coulomb interaction for this Hamiltonian is then an effective interaction  $U_{\text{eff}}$  for Wannier orbitals which is different from the bare Coulomb interaction  $U$  between the *d* electrons. In this way we are actually mimicking the charge-transfer gap by a Mott gap. Such a simplified treatment is quite analogous to the reduction of the two-band *p-d*-hybridized model to a one-band Hubbard model in the context of cuprates.<sup>43</sup> (We note in passing that the Hubbard model and the periodic Anderson model with nearest-neighbor hybridization display a striking similarity near the metal-insulator transition.<sup>44</sup>) Our simplified treatment of the

oxygen  $2p$  bands and the  $p$ - $d$  hybridization should be regarded as a first step towards a full LDA+DMFT investigation of the NiO problem. Within this approximation some of the spectral weight is lost and, in particular, the satellite structure at higher binding energies is ignored. Thus we are not aiming at a calculation of the full spectrum, but rather concentrate on the spectrum near the gap.

Wannier functions can be constructed in different ways. Historically there were attempts<sup>45–47</sup> to produce Wannier functions by a variational procedure, without knowing the actual Bloch functions. Within the context of LDA+DMFT, Andersen and Saha-Dasgupta<sup>48</sup> proposed a way of constructing Wannier functions *a priori* based on  $N$ th-order muffin-tin orbitals (NMO's), which was then applied to  $3d^1$  perovskites<sup>49</sup> and  $\text{Ti}_2\text{O}_3$ .<sup>50</sup> On the other hand, Wannier functions can be calculated straightforwardly by a unitary transformation of a set of Bloch bands. However, due to the *nonuniqueness* of Wannier functions, quantitative computations along this line did not appear until recently. An important progress was made by Marzari and Vanderbilt<sup>51</sup> who devised an optimization procedure to obtain the maximally localized Wannier functions. However, the maximal localization of Wannier functions is not a strict requirement if one is not interested in the orbitals themselves but in a proper representation of the Hamiltonian, which is the case in this work.

In our paper, we follow a procedure proposed recently by Anisimov *et al.*,<sup>52</sup> in which a set of  $d$ -like Wannier functions<sup>42</sup> is constructed in such a way that they (i) preserve the symmetries of the atomic like  $d$  orbitals and (ii) implicitly incorporate the admixture of oxygen  $2p$  orbitals arising from the hybridization effects. The LDA band structure is encoded in a noninteracting Hamiltonian within this basis set of Wannier functions and used as the input for the DMFT study. In the above-mentioned work,<sup>52</sup> calculations were carried out for  $\text{SrVO}_3$  and  $\text{V}_2\text{O}_3$ . Here we extend this scheme to NiO.

From the LDA+DMFT calculation, one can obtain the energy gap, the local magnetic moment, and the electronic spectrum. Since these quantities do not significantly depend on temperature, we compare our results with experimental data at low temperatures and other theoretical results for the ground state.

## B. LDA band structure and construction of Wannier functions

We first perform a standard LDA band calculation using the linear muffin-tin orbital (LMTO) method in atomic sphere approximation<sup>53</sup> with the combined correction term included. The Stuttgart LMTO code version 47 is used for this calculation. Paramagnetic NiO has rocksalt crystal structure, and below  $T_N$  there is a tiny rhombohedral distortion of the cubic unit cell. The lattice constant shows a small increase from about 4.17 Å to 4.20 Å in a temperature range from 7 K to 700 K.<sup>54</sup> Such an increase only causes a small deviation of the bands relatively far away from the Fermi energy, but no noticeable change of the Ni  $3d$ -dominant bands on which we will focus later. Since we will compare our result with the low-temperature experimental data, we choose the lattice constant  $a=4.17$  Å throughout this work.

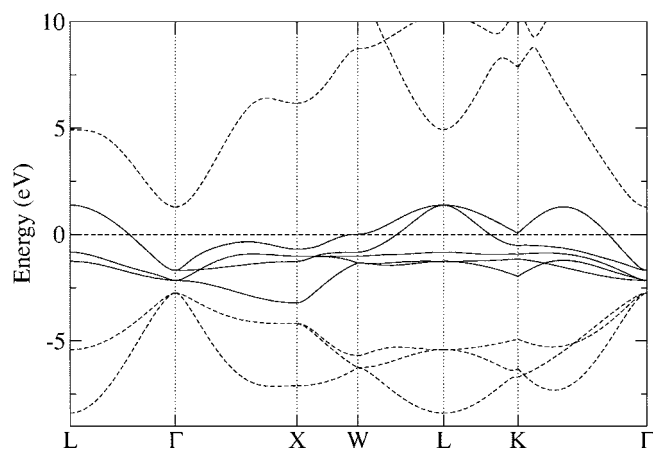


FIG. 1. Nonmagnetic band structure of NiO obtained by the LMTO method; the Fermi energy is set to zero. The five “ $d$ -like” Bloch bands (in solid lines) are used for constructing Wannier functions.

The calculated nonmagnetic band structure of NiO is shown in Fig. 1, and it is in agreement with those published in the literature.<sup>8,11</sup>

Based on the solution of the LDA band problem, we start to construct a set of nonorthogonal Wannier functions centering at a lattice site  $T$ , following Ref. 52,

$$|\tilde{W}_n^T\rangle = \frac{1}{\sqrt{N}} \sum_{\mathbf{k}} e^{i\mathbf{k}\cdot T} |\tilde{W}_{n\mathbf{k}}\rangle = \frac{1}{\sqrt{N}} \sum_{\mathbf{k}} e^{i\mathbf{k}\cdot T} \sum_{i=N_1}^{N_2} |\psi_{i\mathbf{k}}\rangle \langle \psi_{i\mathbf{k}} | \phi_n^{\mathbf{k}} \rangle. \quad (1)$$

Here  $|\psi_{i\mathbf{k}}\rangle$  are the single-particle Bloch states and  $|\phi_n^{\mathbf{k}}\rangle$  are the LMTO basis functions. Furthermore,  $N$  is the number of discretized  $\mathbf{k}$  points in the first Brillouin zone, and  $N_1$  and  $N_2$  determine the range of the Bloch bands to be included in the construction. In the case of NiO we select the five energy bands around the Fermi level, shown by the solid lines in Fig. 1, for our present calculation, and the subscript  $n$  in  $|\phi_n^{\mathbf{k}}\rangle$  enumerates the five Ni  $3d$  LMTO's. These five Bloch bands are dominated by Ni  $3d$  states, but also have considerable contributions from O  $2p$  states resulting from the hybridization effect. The quantities  $|\tilde{W}_{n\mathbf{k}}\rangle$  are simply the Fourier transformation of the real-space Wannier functions  $|\tilde{W}_n^T\rangle$ , but in the multiband case they should be distinguished from eigenfunctions. Hereafter, we refer to  $|\tilde{W}_{n\mathbf{k}}\rangle$  as Wannier functions, too.

So far we have a set of five nonorthogonal Wannier functions with  $d$  symmetry at every  $\mathbf{k}$  point. To orthogonalize them, one needs to calculate the overlap matrix  $O(\mathbf{k})_{nn'}$ ,  $= \langle \tilde{W}_{n\mathbf{k}} | \tilde{W}_{n'\mathbf{k}} \rangle$  and its inverse square root. The orthogonalized Wannier functions are given in the standard way,

$$|W_{n\mathbf{k}}\rangle = \sum_{n'} |\tilde{W}_{n'\mathbf{k}}\rangle (O^{-1/2}(\mathbf{k}))_{n'n}. \quad (2)$$

By using Eqs. (1) and (2) and noticing that  $\hat{H}|\psi_{i\mathbf{k}}\rangle = \varepsilon_i(\mathbf{k})|\psi_{i\mathbf{k}}\rangle$  and  $\langle \phi_n^{\mathbf{k}} | \psi_{i\mathbf{k}} \rangle = c_{ni}(\mathbf{k})$  where  $\varepsilon_i(\mathbf{k})$  and  $c_{ni}(\mathbf{k})$  are the eigenvalues and eigenvectors of the single-particle Kohn-Sham equa-

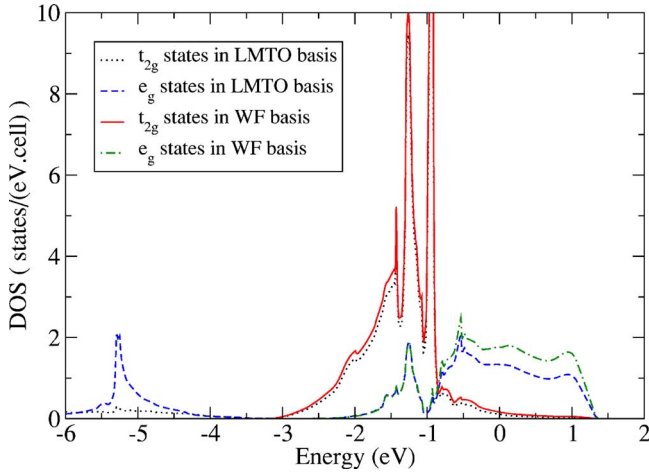


FIG. 2. (Color online).  $t_{2g}$ - and  $e_g$ -resolved LDA DOS in the basis of  $d$ -like Wannier functions ( $t_{2g}$ , red solid curve;  $e_g$ , green dot-dashed curve) and Ni 3d LMTOs ( $t_{2g}$ , black dotted dash curve;  $e_g$ , blue dash curve).

tions, one can express the LDA Hamiltonian matrix within the basis of orthogonalized Wannier functions as

$$\begin{aligned}
 H^{\text{WF}}(\mathbf{k})_{nm'} &= \langle W_{n\mathbf{k}} | \hat{H} | W_{m'\mathbf{k}} \rangle \\
 &= \sum_{m,m'} (O(\mathbf{k})^{-1/2})_{nm} \sum_{i=N_1}^{N_2} c_{mi}(\mathbf{k}) \varepsilon_i(\mathbf{k}) c_{m'i}^*(\mathbf{k}) \\
 &\quad \times (O(\mathbf{k})^{-1/2})_{m'n'}. \quad (3)
 \end{aligned}$$

From the above equation and the relation  $O(\mathbf{k})_{nn'} = \sum_{i=N_1}^{N_2} c_{ni}(\mathbf{k}) c_{n'i}^*(\mathbf{k})$ , it is easy to see that the matrix elements of  $H^{\text{WF}}(\mathbf{k})$  can be built up exclusively in terms of the eigenvalues  $\varepsilon_i(\mathbf{k})$  and eigenvectors  $c_{ni}(\mathbf{k})$  of the LDA single-particle problem. Details of the procedure can be found in Ref. 52.

Next we present the density of states (DOS) of these Wannier functions in Fig. 2 and compare with the Ni 3d LMTO DOS. The Wannier functions constructed in the above procedure have  $d$  symmetry, and therefore in a cubic system as NiO they can also be classified into threefold degenerate  $t_{2g}$  states and twofold degenerate  $e_g$  states. However, one should keep in mind that these Wannier functions are not pure  $d$  states, but rather the antibondinglike states resulting from the hybridization between Ni 3d and O 2p states. This is obvious from Fig. 2, where in the Ni 3d-dominant region the Wannier functions have more spectral weight than LMTO's, the extra spectral weight being due to the contribution of O 2p states. By construction, the bands at higher binding energy with mainly oxygen character are not included in the Wannier functions. Thus, as discussed above, the present scheme does not fully include the O 2p bands and the  $p$ - $d$  hybridization.

### C. Inclusion of correlation effects by LDA+DMFT (QMC)

The single-particle Hamiltonian matrix  $H^{\text{WF}}(\mathbf{k})$  in Wannier function basis must be supplemented with the multior-

bit Coulomb interaction including the local Hund's-rule exchange interaction. In principle,  $H^{\text{WF}}(\mathbf{k})$  should be corrected for the Coulomb interaction that has already been taken into account at the LDA level, yielding a double-counting-free single-particle Hamiltonian matrix  $H_0^{\text{WF}}(\mathbf{k})$ . But in the present case, this effect can be approximated by a trivial shift of the energy (for details see Ref. 33). The full Hamiltonian thus reads

$$\begin{aligned}
 H &= \sum_{\mathbf{k}, n, n', \sigma} H_0^{\text{WF}}(\mathbf{k})_{n,n'} d_{\mathbf{k}n\sigma}^\dagger d_{\mathbf{k}n'\sigma} \\
 &\quad + \frac{1}{2} \sum'_{i, n, n', \sigma, \sigma'} U_{nn'}^{\sigma\sigma'} d_{i n \sigma}^\dagger d_{i n \sigma} d_{i n' \sigma'}^\dagger d_{i n' \sigma'} \\
 &\quad - \frac{1}{2} \sum'_{i, n, n', \sigma} J_{nn'} d_{i n \sigma}^\dagger d_{i n' \sigma}^\dagger d_{i n' \sigma} d_{i n \sigma}. \quad (4)
 \end{aligned}$$

The general interaction  $U_{nn'}^{\sigma\sigma'}$  denotes the Coulomb interaction matrix among different Wannier orbitals. For a cubic system it satisfies the relation  $U_{nn'}^{\sigma\sigma'} = U - 2J(1 - \delta_{nn'}) - J\delta_{\sigma\sigma'}$  to a good approximation. Here  $U$  corresponds to the *effective* interaction between electrons in Wannier orbitals as discussed above and not to the *bare* interaction between the actual  $d$  electrons. The values of the parameters  $U$  and  $J$  are accessible from a constrained LDA calculation. Specifically, from a constrained LDA calculation, the average Coulomb interaction  $\bar{U}$  and the Hund's-rule exchange coupling  $J$  are obtained, which satisfies<sup>33</sup>

$$\bar{U} = \frac{U + (M-1)(U-2J) + (M-1)(U-3J)}{2M-1}, \quad (5)$$

where  $M=5$  is the number of the interacting orbitals. Given  $\bar{U}$  and  $J$  one can thus obtain  $U$  from Eq. (5). Since the constrained LDA calculation has not been performed for the Wannier functions, we take the  $\bar{U}$  value for the LMTO basis from the literature<sup>14</sup> and estimate the value for the Wannier function basis by  $\bar{U}^{\text{WF}} = \bar{U}^{\text{LMTO}}(1-x)^2$  where  $x$  is the admixture of oxygen 2p states into the Wannier functions.<sup>55</sup> For NiO,  $x$  is approximately 0.15 and  $\bar{U}^{\text{LMTO}} = 8$  eV.<sup>14</sup> This means that  $\bar{U}^{\text{WF}} \approx 5.8$  eV. Concerning the  $J$  value it is reasonable to assume that it is only weakly basis dependent, and we just take the LMTO value  $J=1$  eV here. With these considerations we obtain  $U=8$  eV for the Wannier function basis.

We solve the above material-specific model (4) by means of DMFT,<sup>36,37,56</sup> which maps the original lattice model onto a single-impurity model subject to a self-consistent condition. The impurity problem is in turn solved by QMC techniques,<sup>57</sup> yielding an imaginary-time Green function. The maximum-entropy method<sup>58</sup> (MEM) is then used to obtain the physical spectral function on the real frequency axis. We neglect the spin-flip term in Eq. (4) which is known to lead to "minus-sign" problems in QMC simulations,<sup>33</sup> assuming that this term does not play a significant role here. QMC simulations can only be performed at not too low temperatures, since the computation effort scales with  $1/T^3$ .

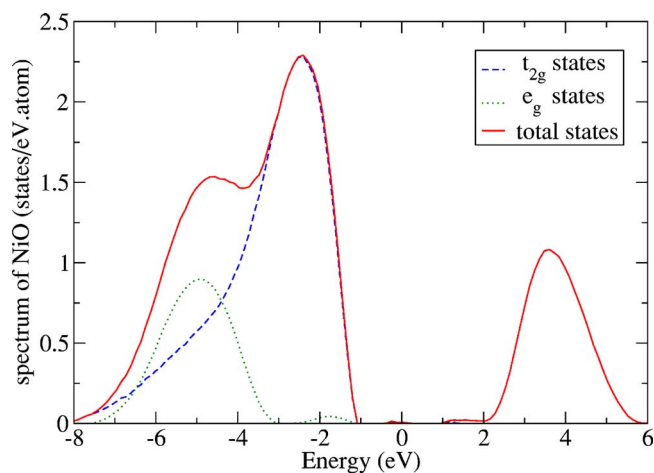


FIG. 3. (Color online). Theoretical energy spectrum of NiO obtained by the LDA+DMFT approach for  $T=1160$  K, and  $U=8$  eV,  $J=1$  eV.  $t_{2g}$  states (blue dashed curve) and  $e_g$  states (green dotted curve) are resolved, and total states (red solid curve) are the sum of the two. Note the curve for total states coincides with that of the unoccupied  $e_g$  states above the chemical potential.

### III. RESULTS AND COMPARISON WITH EXPERIMENT

Our DMFT (QMC) calculations were performed at temperatures  $T=1160$  K, and  $725$  K, respectively. In QMC simulations we used 40 time slices for the former case and 64 for the latter, and in both cases up to  $10^6$  QMC sweeps were made to ensure good convergence. The electronic energy spectrum obtained at temperature  $T=1160$  K for interaction parameters  $U=8$  eV and  $J=1$  eV is shown in Fig. 3. The dominant peak at about  $-2.5$  eV is due to the  $t_{2g}$  bands which are hence completely filled. The  $e_g$  bands are split into lower and upper Hubbard bands. The insulating gap is therefore situated between the occupied  $t_{2g}$  bands and unoccupied  $e_g$  bands.<sup>59</sup> The shoulder between  $-6$  eV and  $-4$  eV originates from the occupied  $e_g$  bands. We understand that this picture differs from the one provided by the cluster model,<sup>6</sup> where both the main peak and side peak are dominated by oxygen character. Indeed, in the present calculation, the hybridization between Ni  $3d$  states and O  $2p$  states is fixed at the LDA level, and a more complete theory of NiO should also allow the  $p$ - $d$  hybridization to evolve under the influence of the interaction among  $d$  electrons. As discussed earlier this requires an explicit inclusion of oxygen states which is not implemented in the present work. Keeping the drawback of the present scheme in mind, we will leave the resolution of this problem to future studies and take the present result as a first approximation. But as shown below, the agreement between the energy spectrum obtained in this calculation and the experiment is already very good.

In Fig. 4 our LDA+DMFT results are compared with data of the combined XPS-BIS experiment by Sawatzky and Allen<sup>7</sup> for the low-temperature AFM phase. Although our calculation was performed for the high-temperature PM phase, a comparison is meaningful since the electronic structure of NiO is almost unaffected by the magnetic phase transition.<sup>25,26</sup> In view of the ambiguity in determining the position of the chemical potential in the insulating gap we

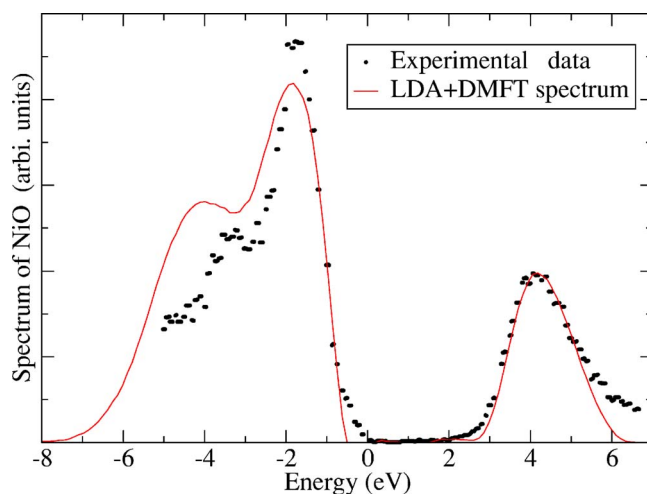


FIG. 4. (Color online). Theoretical spectrum is obtained by the LDA+DMFT approach (red curve) for  $U=8$  eV and  $J=1$  eV at  $T=1160$  K, compared with experimental XPS+BIS data (black dots) after Sawatzky and Allen (Ref. 7). The zero energy point of the theoretical curve is shifted to fit the energy scale of the experimental data.

shifted the spectrum appropriately with respect to the experimental data. The overall agreement between the calculated single-particle spectrum and the experimental data is surprisingly good. Only the shoulder below the main peak is not very well reproduced. It should be noted that the energy spectrum in this region—i.e., far away from the Fermi level—is difficult to obtain accurately due to the limitations imposed by the MEM. On the other hand, matrix element effects, which have so far received little attention in the theoretical calculation of the XPS of NiO, may also play a role here. Although detailed quantitative information on matrix element effects is not available for NiO, it is generally known that in the XPS regime (i) O  $2p$  features become weak relative to the Ni  $3d$  features<sup>60</sup> and (ii) the photoionization cross section of transition metals is suppressed at higher binding energies compared to lower ones.<sup>61,62</sup> The

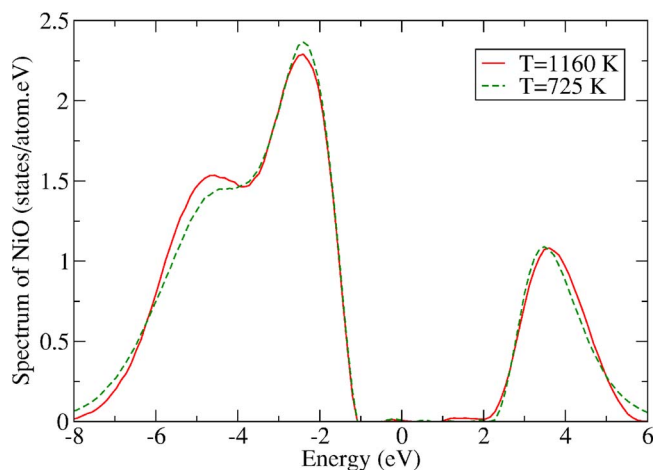


FIG. 5. (Color online). Theoretical spectrum of NiO obtained by the LDA+DMFT approach for  $U=8$  eV,  $J=1$  eV at  $T=1160$  K (red solid curve) and  $T=725$  K (green dashed curve) respectively.

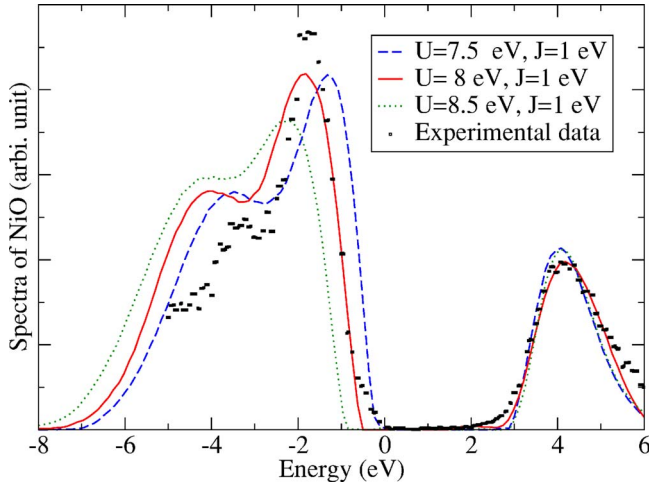


FIG. 6. (Color online) Theoretical spectra obtained by the LDA+DMFT approach for  $U=7.5, 8,$  and  $8.5$  eV (blue dashed, red solid, and green dashed curves, respectively) with fixed  $J=1$  eV and temperature  $T=1160$  K. Experimental XPS+BIS data from Sawatzky and Allen (Ref. 7) are also shown for comparison.

first effect is unlikely to be significant since oxygen features are only contained indirectly in the calculation. The second effect may even improve the agreement further by reducing the weight of the theoretical spectrum at higher binding energies. As a whole, we do not expect matrix element effects to impair the agreement of our results with experiment.

To analyze the effect of the QMC simulation temperature on the spectrum we also performed calculations at  $T=725$  K. The result is shown in Fig. 5 in comparison with that obtained at  $T=1160$  K. Within the numerical error of the QMC method and MEM the spectra at those two temperatures do not show any significant difference. For this reason we expect our results to describe the spectrum of paramagnetic NiO also at even lower temperatures.

It is also interesting to investigate how the spectrum changes when the interaction parameter  $U$  is changed. For this purpose we performed the calculations also for  $U=7.5$  eV and  $8.5$  eV, with fixed  $J=1$  eV, at  $T=1160$  K. The results are shown in Fig. 6, in comparison with that for  $U=8$  eV and the experimental data. Here, to illustrate the change of the insulating gap for different  $U$  values, the positions of the conduction-band peaks were kept fixed. From

Fig. 6 we see that the best agreement with experiment is indeed found for  $U=8$  eV—the value determined from the constrained LDA calculation. The Mott gap is seen to increase roughly linearly with  $U$ . The  $t_{2g}$  and  $e_g$  splitting, however, does not change since it is controlled by the energy  $J$  whose value is fixed here.

In Table I we present our results for the energy gap and the local magnetic moment in comparison with experimental results and the results of other theoretical approaches. Here we measured the energy gap of 4.3 eV as the distance between the half-maximum of the highest valence peak and the conduction peak, respectively, as was done in Ref. 7. The local magnetic moment of  $1.70\mu_B$  is obtained in an indirect way. In experiment the local moment is associated with the spin polarization in the immediate vicinity of the Ni ion. However, in the DMFT calculation the magnetic moment is associated with the Wannier functions. For the parameter  $U=8$  eV and  $J=1$  eV, we find a magnetic moment associated with the Wannier functions as  $m \approx 1.99\mu_B$ .<sup>67</sup> We can then estimate the local magnetic moment associated with the Ni ion by the relation  $m_{\text{loc}}=m(1-x)$  where  $x=0.15$  is again the contribution of O  $2p$  states to Wannier functions.<sup>55</sup> This leads to  $m_{\text{loc}} \approx 1.70\mu_B$  which is in accordance with the measurement and theoretical results obtained for the AFM phase (see Table I). Apparently the value of the local magnetic moment is almost unaffected by the AFM-PM phase transition.

#### IV. CONCLUSION

In this paper we used LDA+DMFT to compute the electronic single-particle spectrum of NiO. Specifically, Wannier functions were constructed corresponding to the five Bloch bands across the Fermi level from the LDA band structure. These were used as the basis for a material-specific multi-band Hubbard-like Hamiltonian. This Hamiltonian was then solved by DMFT using the QMC method as the impurity solver. The electronic spectrum obtained in this way is in very good overall agreement with the experimental XPS+BIS results<sup>7</sup> around the gap region. The energy gap and local magnetic moment obtained by us are in good agreement with experimental results. Taken together with the experimental observation that the long-range AFM order has no significant influence on the valence band photoemission spectra,<sup>25</sup> our result proves that the large insulating gap in

TABLE I. The LSDA, GW, LDA+U, LDA+DMFT (present work), and experimental energy gaps and magnetic moments for NiO.

	LSDA	GW <sup>a</sup>	LDA+U <sup>b</sup>	LDA+DMFT	Expt.
Energy gaps (eV)	0.3	3.7	3.7	4.3	4.3, <sup>c</sup> 4.0 <sup>d</sup>
Magnetic moments ( $\mu_B$ )	1.09	1.83	1.70	1.70	1.64, <sup>e</sup> 1.77, <sup>f</sup> 1.90 <sup>g</sup>

<sup>a</sup>Massidda *et al.* (Ref. 16).

<sup>b</sup>Anisimov *et al.* (Ref. 17).

<sup>c</sup>Sawatzky and Allen (Ref. 7).

<sup>d</sup>Hüfner *et al.* (Ref. 63).

<sup>e</sup>Alperin (Ref. 64).

<sup>f</sup>Fender *et al.* (Ref. 65).

<sup>g</sup>Cheetham and Hope (Ref. 66).

NiO is due to strong electronic correlations in the paramagnetic phase. The magnetic order in NiO is therefore only a secondary effect—i.e., a consequence rather than the origin of the gap. Hence we expect the conduction band photoemission spectra to remain almost unchanged by the AFM long-range order.

In the construction of the *ab initio* Hamiltonian (4), only the five “antibonding” bands (which have mainly Ni 3*d* characters in the LDA calculation) were included, while the three “bonding” bands (which are the mixture of the Ni 3*d* and O 2*p* states, but have more O contributions) below them were neglected. Therefore in the present work the contributions to the Wannier functions from Ni 3*d* and O 2*p* states depend on the LDA results. This means that the valence bands close to the Fermi level have mainly Ni 3*d* character. The insulating gap we obtained is therefore an effective Mott-Hubbard gap between Wannier states. In other words, we used an effective Mott-Hubbard gap to mimic a charge-transfer gap<sup>6,7</sup> or a gap with mixed character.<sup>21,68</sup> Strictly speaking, the gap here is also of mixed character since some amount of oxygen contribution is contained in the Wannier functions. The results obtained by such a treatment are surprisingly good. This may be due to the fact that correlation effects are treated better within DMFT than within any other theoretical approach

available so far, and also because features due to oxygen are rather suppressed in XPS.<sup>60</sup>

In spite of the limitations of the current implementation, we showed that the LDA+DMFT approach which combines first-principles, material-specific information with strong correlation effects is able to deal with late transition-metal monoxides like NiO. A more complete treatment of NiO within the LDA+DMFT approach will require the inclusion of oxygen bands and the *p-d* hybridization. Only in this way can one produce a full spectrum of NiO and identify the satellite structure at high binding energies.

#### ACKNOWLEDGMENTS

We are grateful to V. I. Anisimov, K. Held, V. Eyert, and J. Kunes for valuable discussions. This work was supported by the Deutsche Forschungsgemeinschaft through Sonderforschungsbereich 484, Russian Basic Research Foundation Grants Nos. 05-02-16301, 05-02-17244, the RAS Programs “Quantum macrophysics” and “Strongly correlated electrons in semiconductors, metals, superconductors and magnetic materials,” Dynasty Foundation, a grant of the President of Russia, No. MK-2118.2005.02, and an interdisciplinary grant UB-SB RAS. Computations were performed at the John von Neumann Institut für Computing, Jülich.

\*Current address: Fritz Haber Institute of the Max Planck Society, Faradayweg 4-6, 14195 Berlin, Germany.

<sup>1</sup>L. F. Mattheiss, Phys. Rev. B **5**, 290 (1972).

<sup>2</sup>K. Terakura, T. Oguchi, A. R. Williams, and J. Kübler, Phys. Rev. B **30**, 4734 (1984); K. Terakura, A. R. Williams, T. Oguchi, and J. Kübler, Phys. Rev. Lett. **52**, 1830 (1984).

<sup>3</sup>N. F. Mott, Proc. Phys. Soc., London, Sect. A **62**, 416 (1949).

<sup>4</sup>B. Brandow, Adv. Phys. **26**, 651 (1977).

<sup>5</sup>J. Zaanen, G. A. Sawatzky, and J. W. Allen, Phys. Rev. Lett. **55**, 418 (1985).

<sup>6</sup>A. Fujimori, F. Minami, and S. Sugano, Phys. Rev. B **29**, 5225 (1984); A. Fujimori and F. Minami, Phys. Rev. B **30**, 957 (1984).

<sup>7</sup>G. A. Sawatzky and J. W. Allen, Phys. Rev. Lett. **53**, 2339 (1984).

<sup>8</sup>Z.-X. Shen, R. S. List, D. S. Dessau, B. O. Wells, O. Jepsen, A. J. Arko, R. Bartlett, C. K. Shih, F. Parmigiani, J. C. Huang, and P. A. P. Lindberg, Phys. Rev. B **44**, 3604 (1991).

<sup>9</sup>Z.-X. Shen and D. S. Dessau, Phys. Rep. **253**, 1 (1995).

<sup>10</sup>H. Kühlenbeck, G. Odörfer, R. Jaeger, G. Illing, M. Menges, Th. Mull, H.-J. Freund, M. Pöhlchen, V. Staemmler, S. Witzel, C. Scharfschwerdt, K. Wennemann, T. Liedtke, and M. Neumann, Phys. Rev. B **43**, 1969 (1991).

<sup>11</sup>R. Eder, A. Dorneich, and H. Winter, Phys. Rev. B **71**, 045105 (2005).

<sup>12</sup>L.-C. Duda, T. Schmitt, M. Magnuson, J. Forsberg, A. Olsson, J. Nordgren, K. Okada, and A. Kotani, Phys. Rev. Lett. **96**, 067402 (2006).

<sup>13</sup>A. Svane and O. Gunnarsson, Phys. Rev. Lett. **65**, 1148 (1991).

<sup>14</sup>V. I. Anisimov, J. Zaanen, and O. K. Andersen, Phys. Rev. B **44**,

943 (1991).

<sup>15</sup>F. Aryasetiawan and O. Gunnarsson, Phys. Rev. Lett. **74**, 3221 (1995).

<sup>16</sup>S. Massidda, A. Continenza, M. Posternak, and A. Baldereschi, Phys. Rev. B **55**, 13494 (1997).

<sup>17</sup>V. I. Anisimov, I. V. Solovyev, M. A. Korotin, M. T. Czyżyk, and G. A. Sawatzky, Phys. Rev. B **48**, 16929 (1993).

<sup>18</sup>V. I. Anisimov, P. Kuiper, and J. Nordgren, Phys. Rev. B **50**, 8257 (1994).

<sup>19</sup>J. Hugel and M. Kamal, J. Phys.: Condens. Matter **9**, 647 (1997).

<sup>20</sup>A. B. Shick, A. I. Liechtenstein, and W. E. Pickett, Phys. Rev. B **60**, 10763 (1999).

<sup>21</sup>O. Bengone, M. Alouani, P. Blöchl, and J. Hugel, Phys. Rev. B **62**, 16392 (2000).

<sup>22</sup>S. V. Faleev, M. van Schilfgaarde, and T. Kotani, Phys. Rev. Lett. **93**, 126406 (2004).

<sup>23</sup>J.-L. Li, G.-M. Rignanese, and S. G. Louie, Phys. Rev. B **71**, 193102 (2005).

<sup>24</sup>F. Manghi, C. Calandra, and S. Ossicini, Phys. Rev. Lett. **73**, 3129 (1994).

<sup>25</sup>O. Tjernberg, S. Söderholm, G. Chiaia, R. Girard, U. O. Karlsson, H. Nylén, and I. Lindau, Phys. Rev. B **54**, 10245 (1996).

<sup>26</sup>W. Jauch and M. Reehuis, Phys. Rev. B **70**, 195121 (2004).

<sup>27</sup>J. C. Slater, Phys. Rev. **82**, 538 (1951).

<sup>28</sup>V. I. Anisimov, A. I. Poteryaev, M. A. Korotin, A. O. Anokhin, and G. Kotliar, J. Phys.: Condens. Matter **9**, 7359 (1997).

<sup>29</sup>A. I. Liechtenstein and M. I. Katsnelson, Phys. Rev. B **57**, 6884 (1998).

<sup>30</sup>I. A. Nekrasov, K. Held, N. Blümer, A. I. Poteryaev, V. I. Anisimov, and D. Vollhardt, Eur. Phys. J. B **18**, 55 (2000).

- <sup>31</sup>K. Held, I. A. Nekrasov, N. Blümer, V. I. Anisimov, and D. Vollhardt, *Int. J. Mod. Phys. B* **15**, 2611 (2001); K. Held, I. A. Nekrasov, G. Keller, V. Eyert, N. Blümer, A. K. McMahan, R. T. Scalettar, T. Pruschke, V. I. Anisimov, and D. Vollhardt, in *Quantum Simulations of Complex Many-Body Systems: From Theory to Algorithms*, edited by J. Grotendorst, D. Marks, and A. Muramatsu, NIC Series, Vol. 10 (NIC Directors, Forschungszentrum Jülich, 2002), pp. 175–209.
- <sup>32</sup>A. I. Lichtenstein, M. I. Katsnelson, and G. Kotliar, in *Electron Correlations and Materials Properties*, 2nd ed., edited by A. Gonis, N. Kioussis, and M. Ciftan (Kluwer Academic/Plenum, New York, 2002), p. 428.
- <sup>33</sup>K. Held, I. A. Nekrasov, G. Keller, V. Eyert, N. Blumer, A. K. McMahan, R. T. Scalettar, Th. Pruschke, V. I. Anisimov, and D. Vollhardt, *Psi-k Newsletter* **56**, 65 (2003), [http://psi-k.dl.ac.uk/newsletters/News\\_56/Highlight\\_56.pdf](http://psi-k.dl.ac.uk/newsletters/News_56/Highlight_56.pdf)
- <sup>34</sup>G. Kotliar, S. Y. Savrasov, K. Haule, V. S. Oudovenko, O. Parcollet, and C. A. Marianetti, *Rev. Mod. Phys.* **78**, 865 (2006).
- <sup>35</sup>K. Held, cond-mat/0511293 (unpublished).
- <sup>36</sup>A. Georges, G. Kotliar, W. Krauth, and M. J. Rozenberg, *Rev. Mod. Phys.* **68**, 13 (1996).
- <sup>37</sup>G. Kotliar and D. Vollhardt, *Phys. Today* **57**(3), 53 (2004).
- <sup>38</sup>A. Georges and G. Kotliar, *Phys. Rev. B* **45**, 6479 (1992).
- <sup>39</sup>M. Jarrell, *Phys. Rev. Lett.* **69**, 168 (1992).
- <sup>40</sup>W. Metzner and D. Vollhardt, *Phys. Rev. Lett.* **62**, 324 (1989).
- <sup>41</sup>S. Y. Savrasov and G. Kotliar, *Phys. Rev. Lett.* **90**, 056401 (2003).
- <sup>42</sup>G. H. Wannier, *Phys. Rev.* **52**, 191 (1937).
- <sup>43</sup>E. Dagotto, *Rev. Mod. Phys.* **66**, 763 (1994).
- <sup>44</sup>K. Held and R. Bulla, *Eur. Phys. J. B* **17**, 7 (2000).
- <sup>45</sup>G. F. Koster, *Phys. Rev.* **89**, 67 (1953).
- <sup>46</sup>G. Parzen, *Phys. Rev.* **89**, 237 (1953).
- <sup>47</sup>W. Kohn, *Phys. Rev. B* **7**, 4388 (1973).
- <sup>48</sup>O. K. Andersen and T. Saha-Dasgupta, *Phys. Rev. B* **62**, R16219 (2000).
- <sup>49</sup>E. Pavarini, S. Biermann, A. Poteryaev, A. I. Lichtenstein, A. Georges, and O. K. Andersen, *Phys. Rev. Lett.* **92**, 176403 (2004).
- <sup>50</sup>A. I. Poteryaev, A. I. Lichtenstein, and G. Kotliar, *Phys. Rev. Lett.* **93**, 086401 (2004).
- <sup>51</sup>N. Marzari and D. Vanderbilt, *Phys. Rev. B* **56**, 12847 (1997).
- <sup>52</sup>V. I. Anisimov, D. E. Kondakov, A. V. Kozhevnikov, I. A. Nekrasov, Z. V. Pchelkina, J. W. Allen, S.-K. Mo, H.-D. Kim, P. Metcalf, S. Suga, A. Sekiyama, G. Keller, I. Leonov, X. Ren, and D. Vollhardt, *Phys. Rev. B* **71**, 125119 (2005).
- <sup>53</sup>O. K. Andersen, *Phys. Rev. B* **12**, 3060 (1975); H. L. Skriver, *The LMTO Method, Springer Series in Solid State Science*, Vol. 41, (Springer, New York, 1984).
- <sup>54</sup>L. C. Bartel and B. Morosin, *Phys. Rev. B* **3**, 1039 (1971).
- <sup>55</sup>V. I. Anisimov (private communication).
- <sup>56</sup>D. Vollhardt, K. Held, G. Keller, R. Bulla, Th. Pruschke, I. A. Nekrasov, and V. I. Anisimov, *J. Phys. Soc. Jpn.* **74**, 136 (2005).
- <sup>57</sup>J. E. Hirsch and R. M. Fye, *Phys. Rev. Lett.* **56**, 2521 (1986).
- <sup>58</sup>M. Jarrell and J. E. Gubernatis, *Phys. Rep.* **269**, 133 (1996).
- <sup>59</sup>The finite but very low spectral weight in the gap between 1 and 2 eV appears to be an artifact of the maximum-entropy method.
- <sup>60</sup>D. E. Eastman and J. L. Freeouf, *Phys. Rev. Lett.* **34**, 395 (1975).
- <sup>61</sup>T.-U. Nahm, M. Han, S.-J. Oh, J.-H. Park, J. W. Allen, and S.-M. Chung, *Phys. Rev. Lett.* **70**, 3663 (1993).
- <sup>62</sup>W. Speier, J. C. Fuggle, P. Durham, R. Zeller, R. J. Blake, and P. Sterne, *J. Phys. C* **21**, 2621 (1988).
- <sup>63</sup>S. Hüfner, J. Osterwalder, T. Riesterer, and F. Hulliger, *Solid State Commun.* **52**, 793 (1984).
- <sup>64</sup>H. A. Alperin, *J. Phys. Soc. Jpn.* **17**, Suppl. B (3), 12 (1962).
- <sup>65</sup>B. E. F. Fender, A. J. Jacobson, and F. A. Wegwood, *J. Chem. Phys.* **48**, 990 (1968).
- <sup>66</sup>A. K. Cheetham and D. A. O. Hope, *Phys. Rev. B* **27**, 6964 (1983).
- <sup>67</sup>To obtain a local magnetic moment in the PM phase whose value is close to the maximal value is a nontrivial result. This value becomes smaller as  $U$  and  $J$  are reduced.
- <sup>68</sup>T. M. Schuler, D. L. Ederer, S. Itza-Ortiz, G. T. Woods, T. A. Callcott, and J. C. Woicik, *Phys. Rev. B* **71**, 115113 (2005).